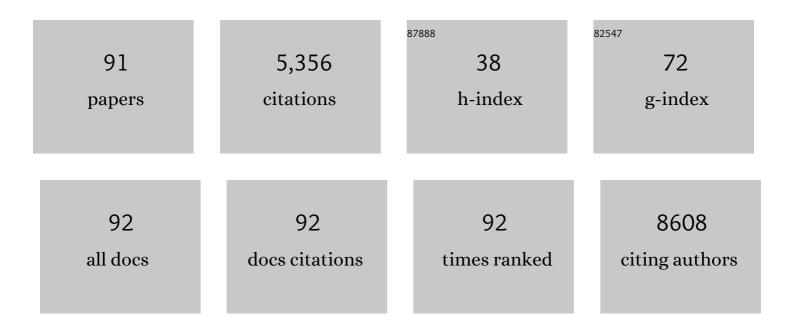
## Jianxin Geng

List of Publications by Year in descending order

Source: https://exaly.com/author-pdf/7385737/publications.pdf Version: 2024-02-01



IIANYIN GENC

#	Article	IF	CITATIONS
1	Singleâ€Atom Catalyst Aggregates: Sizeâ€Matching is Critical to Electrocatalytic Performance in Sulfur Cathodes. Advanced Science, 2022, 9, e2103773.	11.2	40
2	Covalently Grafting Sulfur-Containing Polymers to Carbon Nanotubes Enhances the Electrochemical Performance of Sulfur Cathodes. ACS Applied Polymer Materials, 2022, 4, 939-949.	4.4	13
3	Encoding Enantiomeric Molecular Chiralities on Graphene Basal Planes. Angewandte Chemie - International Edition, 2022, 61, .	13.8	10
4	Zeolitic Imidazolate Framework-Derived Co-Fe@NC for Rechargeable Hybrid Sodium–Air Battery with a Low Voltage Gap and Long Cycle Life. ACS Applied Energy Materials, 2022, 5, 1662-1671.	5.1	8
5	Surface reconstruction establishing Mott-Schottky heterojunction and built-in space-charging effect accelerating oxygen evolution reaction. Nano Research, 2022, 15, 2952-2960.	10.4	15
6	Coaxially grafting conjugated microporous polymers containing single-atom cobalt catalysts to carbon nanotubes enhances sulfur cathode reaction kinetics. Chemical Engineering Journal, 2022, 444, 136546.	12.7	24
7	Covalently grafting conjugated porous polymers to MXene offers a two-dimensional sandwich-structured electrocatalytic sulfur host for lithium–sulfur batteries. Chemical Engineering Journal, 2022, 446, 137365.	12.7	25
8	Carbonâ€Based Materials as Lithium Hosts for Lithium Batteries. Chemistry - A European Journal, 2022, 28, .	3.3	9
9	Aluminumâ^'lithium alloy as a stable and reversible anode for lithium batteries. Electrochimica Acta, 2021, 368, 137626.	5.2	33
10	lce-Templated Large-Scale Preparation of Two-Dimensional Sheets of Conjugated Polymers: Thickness-Independent Flexible Supercapacitance. ACS Nano, 2021, 15, 8870-8882.	14.6	39
11	Regulating Lithium Plating and Stripping by Using Vertically Aligned Graphene/CNT Channels Decorated with ZnO Particles. Chemistry - A European Journal, 2021, 27, 15706-15715.	3.3	13
12	A Conjugated Porous Polymer Complexed with a Single-Atom Cobalt Catalyst as An Electrocatalytic Sulfur Host for Enhancing Cathode Reaction Kinetics. Energy Storage Materials, 2021, 41, 14-23.	18.0	51
13	Agarose-Based Hierarchical Porous Carbons Prepared with Gas-Generating Activators and Used in High-Power Density Supercapacitors. Energy & Fuels, 2021, 35, 19775-19783.	5.1	5
14	Sulfur covalently bonded to porous graphitic carbon as an anode material for lithium-ion capacitors with high energy storage performance. Journal of Materials Chemistry A, 2020, 8, 62-68.	10.3	31
15	Unveiling the Origin of Catalytic Sites of Pt Nanoparticles Decorated on Oxygen-Deficient Vanadium-Doped Cobalt Hydroxide Nanosheet for Hybrid Sodium–Air Batteries. ACS Applied Energy Materials, 2020, 3, 7464-7473.	5.1	9
16	Recent Advances in Polymer-Based Photothermal Materials for Biological Applications. ACS Applied Polymer Materials, 2020, 2, 4273-4288.	4.4	65
17	State-of-the-Art Applications of 2D Nanomaterials in Energy Storage. ACS Symposium Series, 2020, , 253-293.	0.5	5
18	Electrocatalysis: Kinetic Enhancement of Sulfur Cathodes by Nâ€Doped Porous Graphitic Carbon with Bound VN Nanocrystals (Small 48/2020). Small, 2020, 16, 2070261.	10.0	2

JIANXIN GENG

#	Article	IF	CITATIONS
19	Kinetic Enhancement of Sulfur Cathodes by Nâ€Đoped Porous Graphitic Carbon with Bound VN Nanocrystals. Small, 2020, 16, e2004950.	10.0	64
20	Tandem chemical modification/mechanical exfoliation of graphite: Scalable synthesis of high-quality, surface-functionalized graphene. Carbon, 2019, 145, 668-676.	10.3	57
21	Covalent Confinement of Sulfur Copolymers onto Graphene Sheets Affords Ultrastable Lithium–Sulfur Batteries with Fast Cathode Kinetics. ACS Applied Materials & Interfaces, 2019, 11, 13234-13243.	8.0	50
22	Rational design of sulfur-containing composites for high-performance lithium–sulfur batteries. APL Materials, 2019, 7, .	5.1	30
23	Synthesis of a Macroporous Conjugated Polymer Framework: Iron Doping for Highly Stable, Highly Efficient Lithium–Sulfur Batteries. ACS Applied Materials & Interfaces, 2019, 11, 3087-3097.	8.0	52
24	The preparation and functional applications of carbon nanomaterial/conjugated polymer composites. Composites Communications, 2019, 12, 64-73.	6.3	55
25	Covalent bonding of sulfur nanoparticles to unzipped multiwalled carbon nanotubes for high-performance lithium–sulfur batteries. Nanotechnology, 2019, 30, 024001.	2.6	22
26	High-performance solution-based CdS-conjugated hybrid polymer solar cells. RSC Advances, 2018, 8, 18051-18058.	3.6	26
27	Macroporous Graphene Thin Films as Electrochemical Electrodes: Enhancing the Sensitivity for Detection of Metal lons. Journal of Nanoscience and Nanotechnology, 2018, 18, 4100-4105.	0.9	3
28	Tuning the Surface Properties of Graphene Oxide by Surface-Initiated Polymerization of Epoxides: An Efficient Method for Enhancing Gas Separation. ACS Applied Materials & Interfaces, 2017, 9, 4998-5005.	8.0	53
29	Enhanced Photothermal Bactericidal Activity of the Reduced Graphene Oxide Modified by Cationic Water-Soluble Conjugated Polymer. ACS Applied Materials & Interfaces, 2017, 9, 5382-5391.	8.0	81
30	Core–Shell Structured Polyamide 66 Nanofibers with Enhanced Flame Retardancy. ACS Omega, 2017, 2, 2665-2671.	3.5	31
31	Fabrication of polythiophene patterns through blending of a thermally curable polythiophene with poly(methyl methacrylate) and selective thermal curation. Chinese Journal of Polymer Science (English Edition), 2017, 35, 422-433.	3.8	4
32	Graphene Oxide Facilitates Solventâ€Free Synthesis of Wellâ€Dispersed, Faceted Zeolite Crystals. Angewandte Chemie - International Edition, 2017, 56, 14090-14095.	13.8	41
33	Graphene Oxide Facilitates Solventâ€Free Synthesis of Wellâ€Dispersed, Faceted Zeolite Crystals. Angewandte Chemie, 2017, 129, 14278-14283.	2.0	18
34	Tuning the morphologies of fluorine-doped tin oxides in the three-dimensional architecture of graphene for high-performance lithium-ion batteries. Nanotechnology, 2017, 28, 395404.	2.6	20
35	Lightweight and Ultrastrong Polymer Foams with Unusually Superior Flame Retardancy. ACS Applied Materials & Interfaces, 2017, 9, 26392-26399.	8.0	66
36	Towards efficient and cost-effective inverted hybrid organic solar cells using inorganic semiconductor in the active layer. Applied Nanoscience (Switzerland), 2017, 7, 747-752.	3.1	11

JIANXIN GENG

#	Article	IF	CITATIONS
37	Controlled Growth of Well-Defined Conjugated Polymers from the Surfaces of Multiwalled Carbon Nanotubes: Photoresponse Enhancement via Charge Separation. ACS Nano, 2016, 10, 5189-5198.	14.6	34
38	Conjunction of Conducting Polymer Nanostructures with Macroporous Structured Graphene Thin Films for High-Performance Flexible Supercapacitors. ACS Applied Materials & Interfaces, 2016, 8, 11711-11719.	8.0	57
39	Cellulose Tailored Anatase TiO <sub>2</sub> Nanospindles in Three-Dimensional Graphene Composites for High-Performance Supercapacitors. ACS Applied Materials & Interfaces, 2016, 8, 12165-12175.	8.0	91
40	Three-dimensional porous carbon composites containing high sulfur nanoparticle content for high-performance lithium–sulfur batteries. Nature Communications, 2016, 7, 10601.	12.8	637
41	Controllable Fabrication of Transparent Macroporous Graphene Thin Films and Versatile Applications as a Conducting Platform. Advanced Functional Materials, 2015, 25, 4334-4343.	14.9	25
42	Graphene Oxide: A Versatile Agent for Polyimide Foams with Improved Foaming Capability and Enhanced Flexibility. Chemistry of Materials, 2015, 27, 4358-4367.	6.7	66
43	Tunable Functionalization of Graphene Oxide Sheets through Surface-Initiated Cationic Polymerization. Macromolecules, 2015, 48, 994-1001.	4.8	60
44	Synergetic deoxy reforming of cellulose and fatty acid esters for liquid hydrocarbon-rich oils. Bioresource Technology, 2015, 196, 217-224.	9.6	10
45	Fluorine-Doped SnO <sub>2</sub> @Graphene Porous Composite for High Capacity Lithium-Ion Batteries. Chemistry of Materials, 2015, 27, 4594-4603.	6.7	175
46	Graphene Wrapped TiO <sub>2</sub> Based Catalysts with Enhanced Photocatalytic Activity. Advanced Materials Interfaces, 2014, 1, 1300150.	3.7	65
47	The enhanced photothermal effect of graphene/conjugated polymer composites: photoinduced energy transfer and applications in photocontrolled switches. Chemical Communications, 2014, 50, 14345-14348.	4.1	93
48	Templateâ€Free Preparation of Volvoxâ€like Cd <sub><i>x</i></sub> Zn <sub>1â^'<i>x</i></sub> S Nanospheres with Cubic Phase for Efficient Photocatalytic Hydrogen Production. Chemistry - an Asian Journal, 2014, 9, 811-818.	3.3	47
49	Scalable and facile preparation of graphene aerogel for air purification. RSC Advances, 2014, 4, 4843.	3.6	47
50	Enhanced electrochemical response for mercury ion detection based on poly(3-hexylthiophene) hybridized with multi-walled carbon nanotubes. RSC Advances, 2014, 4, 25051.	3.6	27
51	Synthesis of graphene/Ni–Al layered double hydroxide nanowires and their application as an electrode material for supercapacitors. Journal of Materials Chemistry A, 2014, 2, 5060.	10.3	114
52	Composite Films of Poly(3-hexylthiophene) Grafted Single-Walled Carbon Nanotubes for Electrochemical Detection of Metal Ions. ACS Applied Materials & Interfaces, 2014, 6, 7686-7694.	8.0	39
53	A dual-fluorescent composite of graphene oxide and poly(3-hexylthiophene) enables the ratiometric detection of amines. Chemical Science, 2014, 5, 3130.	7.4	42
54	Scalable preparation of three-dimensional porous structures of reduced graphene oxide/cellulose composites and their application in supercapacitors. Carbon, 2013, 62, 501-509.	10.3	202

JIANXIN GENG

#	Article	IF	CITATIONS
55	Enhanced photoresponse of large-sized photoactive graphene composite films based on water-soluble conjugated polymers. Chemical Communications, 2013, 49, 5538.	4.1	37
56	Deposition SnO <sub>2</sub> /Nitrogen-Doped Graphene Nanocomposites on the Separator: A New Type of Flexible Electrode for Energy Storage Devices. ACS Applied Materials & Interfaces, 2013, 5, 12148-12155.	8.0	66
57	Selective surface functionalization at regions of high local curvature in graphene. Chemical Communications, 2013, 49, 677-679.	4.1	135
58	Humidity Effects on the Wetting Characteristics of Poly( <i>N</i> -isopropylacrylamide) during a Lower Critical Solution Transition. Langmuir, 2013, 29, 8116-8124.	3.5	12
59	Preparation of fractal-like structures of insoluble polythiophene via solvent vapor annealing of solid thermocleavable polythiophene films and subsequent thermal curing. Polymer Journal, 2013, 45, 813-818.	2.7	2
60	Multiple-bilayered RGO–porphyrin films: from preparation to application in photoelectrochemical cells. Journal of Materials Chemistry, 2012, 22, 18879.	6.7	48
61	Grafting P3HT brushes on GO sheets: distinctive properties of the GO/P3HT composites due to different grafting approaches. Journal of Materials Chemistry, 2012, 22, 21583.	6.7	51
62	Graphite oxide: a selective and highly efficient oxidant of thiols and sulfides. Organic and Biomolecular Chemistry, 2011, 9, 7292.	2.8	224
63	Effect of the Exposure Time of Hydrazine Vapor on the Reduction of Graphene Oxide Films. Journal of Nanoscience and Nanotechnology, 2011, 11, 5959-5964.	0.9	7
64	A Simple Approach for Preparing Transparent Conductive Graphene Films Using the Controlled Chemical Reduction of Exfoliated Graphene Oxide in an Aqueous Suspension. Journal of Physical Chemistry C, 2010, 114, 14433-14440.	3.1	109
65	Porphyrin Functionalized Graphene Sheets in Aqueous Suspensions: From the Preparation of Graphene Sheets to Highly Conductive Graphene Films. Journal of Physical Chemistry C, 2010, 114, 8227-8234.	3.1	309
66	Preparation of graphene relying on porphyrin exfoliation of graphite. Chemical Communications, 2010, 46, 5091.	4.1	154
67	Enhanced Solarâ€Cell Efficiency in Bulkâ€Heterojunction Polymer Systems Obtained by Nanoimprinting with Commercially Available AAO Membrane Filters. Small, 2009, 5, 2139-2143.	10.0	118
68	Enhanced field emission of an electric field assisted single-walled carbon nanotube assembly in colloid interstices. Carbon, 2009, 47, 1555-1560.	10.3	12
69	Effect of Cation Size on Solid Polymer Electrolyte Based Dye-Sensitized Solar Cells. Langmuir, 2009, 25, 3276-3281.	3.5	92
70	Enhanced Electrical Conductivities of Transparent Double-Walled Carbon Nanotube Network Films by Post-treatment. Journal of Physical Chemistry C, 2009, 113, 13658-13663.	3.1	28
71	Layer-by-layer assembly of graphene and gold nanoparticles by vacuum filtration and spontaneous reduction of gold ions. Chemical Communications, 2009, , 2174.	4.1	393
72	Effect of SWNT Defects on the Electron Transfer Properties in P3HT/SWNT Hybrid Materials. Advanced Functional Materials, 2008, 18, 2659-2665.	14.9	102

Jianxin Geng

#	Article	IF	CITATIONS
73	Synthesis of SWNT Rings by Noncovalent Hybridization of Porphyrins and Single-Walled Carbon Nanotubes. Journal of Physical Chemistry C, 2008, 112, 12264-12271.	3.1	46
74	Fabrication of well-aligned SWNT arrays using colloidal self-assembly. , 2008, , .		0
75	A simple and low-temperature hydrothermal route for the synthesis of tubular α-FeOOH. Materials Letters, 2007, 61, 4794-4796.	2.6	36
76	Influence of Single-Walled Carbon Nanotubes Induced Crystallinity Enhancement and Morphology Change on Polymer Photovoltaic Devices. Journal of the American Chemical Society, 2006, 128, 16827-16833.	13.7	226
77	Crystal structure and morphology of phenyl-capped tetraaniline in the leucoemeraldine oxidation state. Journal of Polymer Science, Part B: Polymer Physics, 2006, 44, 764-769.	2.1	28
78	Phase structure and transition behavior of a liquid crystal 5-{[(4′-heptoxy-4-biphenylyl)oxy]carbonyl}-1-pentyne. Journal of Molecular Liquids, 2006, 124, 96-101.	4.9	3
79	An environment-friendly microemulsion approach to α-FeOOH nanorods at room temperature. Materials Research Bulletin, 2006, 41, 2238-2243.	5.2	36
80	Phase transition behavior and structure of the thermotropic liquid crystal 6-{[(4′-{[(undecyl)carbonyl]oxy}biphenyl-4yl)carbonyl]oxy}-1-hexyne. Crystal Research and Technology, 2006, 41, 914-918.	1.3	3
81	A study of NiZnCu-ferrite/SiO2 nanocomposites with different ferrite contents synthesized by sol–gel method. Journal of Magnetism and Magnetic Materials, 2005, 292, 304-309.	2.3	18
82	Preparation of Ni0.65Zn0.35Cu0.1Fe1.9O4/SiO2 nanocomposites by sol–gel method. Journal of Crystal Growth, 2004, 262, 415-419.	1.5	12
83	Electric-field-induced molecular alignment of side-chain liquid-crystalline polyacetylenes containing biphenyl mesogens. Journal of Polymer Science, Part B: Polymer Physics, 2004, 42, 1333-1341.	2.1	14
84	Preparation of nanocrystalline NiZnCu ferrite particles by sol–gel method and their magnetic properties. Journal of Magnetism and Magnetic Materials, 2004, 277, 84-89.	2.3	70
85	Structure and liquid crystalline properties of 5-[(4′-heptoxy-4-biphenylyl)carbonyloxy]-1-pentyne. Liquid Crystals, 2004, 31, 71-79.	2.2	5
86	Liquid crystal properties of a mesogenic polyacetylene, poly(11-[(4′-heptoxy-4-biphenylyl)carbonyloxy]-1-undecyne). Liquid Crystals, 2004, 31, 271-277.	2.2	3
87	Shear induced molecular alignments of a side-chain liquid crystalline polyacetylene containing biphenyl mesogens. Polymer, 2003, 44, 8095-8102.	3.8	23
88	HIGH ORDER LIQUID CRYSTALLINE STRUCTURE OF POLY(11-{[(4′-HEPTYLOXY-4-BIPHENYLYL)CARBONYL]OXY}-1-UNDECYNE). Molecular Crystals and Liquid Crystals, 2003, 399, 17-28.	0.9	11
89	Crystal Structure of 11-{[(4′-Heptoxy-4-Biphenylyl) Carbonyl] Oxy}-1-Undecyne. Molecular Crystals and Liquid Crystals, 2002, 383, 115-130.	0.9	5
90	Phase Transition and Transition Kinetics of a Thermotropic Poly(amideâ^'imide) Derived from 70 Pyromellitic Dianhydride, 30 Terephthaloyl Chloride, and 1,3-Bis[4-(4â€~-aminophenoxy)cumyl]benzene. Macromolecules, 2001, 34, 8710-8719.	4.8	6

#	Article	IF	CITATIONS
91	Encoding Enantiomeric Molecular Chiralities on Graphene Basal Planes. Angewandte Chemie, 0, , .	2.0	0